An Intelligent WSN Framework for Early Warning and Safety Monitoring in Underground Mines

L PRASHANTH KUMAR[1], P LOKESWARA RAO[2], B NAVAJEEVAN[3]
[1, 2,3,]Assistant Professor, Department of Mining Engineering, Anu Bose Institute of Technology for women's, KSP Road, New Paloncha, Bhadradri Kothagudem District, Telangana (TS), 507115

Abstract — Underground coal and mineral extraction exposes workers to explosive and toxic gases, oxygen deficiency, heat, strata failure, and communication problems. Conventional manual sampling and cabled telemetry offer information that is sparse, delayed, and vulnerable to failure. This paper describes the design and simulation-based evaluation of a wireless sensor network (WSN) for real-time monitoring of safety and environmental conditions in underground mines. The system integrates sensing nodes for gases (CH_4, CO, CO_2, O_2), microclimate conditions (temperature, humidity, airflow), and strata convergence with an IEEE 802.15.4 multi-hop mesh backbone, an underground gateway, and a surface control-room server. Embedded signal filtering, adaptive sampling, and a two-out-of-three confirmation rule help limit false alarms, while a weighted composite risk index combines all parameters into a single graded alert. The study develops analytical models of tunnel path loss, multi-hop packet delivery, node energy use, detection delay, methane dilution, and Atkinson's ventilation law. Monte Carlo simulations of a 2 km roadway show that the mesh topology maintains a packet delivery ratio of 72.9% at 2 km, compared with 51.5% for a single-path tree; the star topology fails beyond approximately 100 m. During a simulated methane build-up, the adaptive WSN detected the 1.0% warning threshold after a mean delay of 7.4 s, versus 92.0 s for wired telemetry polling every 60 s and 15.9 min for manual rounds conducted every 30 minutes. It also lowered the expected false-alarm rate from 2.88 to 0.009 per node per day. These findings suggest that a properly engineered WSN can deliver faster, denser, and more resilient hazard awareness than conventional monitoring, while supporting ventilation management and rescue operations.

Keywords: Wireless sensor network, underground mine safety, methane monitoring, environmental monitoring, IEEE 802.15.4 mesh, mine ventilation, risk index

This is an open access article under the creative commons license https://creativecommons.org/licenses/by-nc-nd/4.0/
CC BY-NC-ND 4.0

I. INTRODUCTION

1.1 Background of the Mining Industry

Mining supplies the coal, metals and industrial minerals on which power generation, construction, manufacturing and transport depend. As surface deposits are depleted, production is shifting to deeper and more geologically complex underground workings, where roadways extend for kilometres from the shaft or portal, and the working environment is continuously altered by blasting, cutting, ventilation changes and strata movement [1]. In such environments the miner depends on a chain of engineered controls — ventilation, gas monitoring, ground support and communication — all of which must remain reliable in a hot, humid, dusty, confined and potentially explosive atmosphere.

1.2 Importance of Safety and Environmental Monitoring

Underground mine disasters such as methane and coal-dust explosions, mine fires, inrushes, roof falls and asphyxiation are typically preceded by measurable changes in gas concentration, temperature, airflow or ground deformation. Continuous monitoring of these parameters therefore converts a reactive safety culture into a predictive one: early warning gives time to withdraw personnel, de-energise equipment and adjust ventilation. Environmental monitoring also supports occupational health compliance, ventilation economy and regulatory reporting.

1.3 Existing Challenges in Mining Operations

Conventional monitoring relies on periodic manual measurements with hand-held detectors and on cabled sensors connected to a surface scanning system. Manual rounds leave long intervals in which conditions are unobserved. Cabled systems are expensive to extend, are routinely cut by blasting, roof falls and moving machinery, and are difficult to re-route as faces advance. Radio propagation in tunnels is demanding because of multipath, waveguide effects, bends, rough walls, roof supports and vehicles, and devices must satisfy intrinsic-safety constraints that limit power and storage energy [3], [4].

1.4 Research Problem and Motivation

Wireless sensor networks (WSNs) — large numbers of low-cost, battery-powered nodes that sense, process and relay data cooperatively [2] — offer a way of densifying monitoring points, avoiding vulnerable cabling and re-deploying quickly as the mine advances. However, a mine-grade WSN must reconcile conflicting demands: reliable multi-hop delivery along a long linear tunnel, low latency for alarm traffic, long node life under intrinsic-safety power limits, and a low false-alarm rate so that alarms remain credible. This paper is motivated by the need for a quantified, design-level understanding of these trade-offs.

1.5 Research Objectives and Contributions

The principal contributions of this work are:

- A layered WSN architecture integrating gas, microclimate, strata and personnel-tracking nodes with a mesh backbone, an underground gateway and a surface server.
- Analytical models for tunnel path loss, hop-by-hop packet delivery, node energy and network lifetime, and alarm detection delay.
- An embedded filtering, adaptive-sampling and two-out-of-three confirmation scheme that shortens detection delay while suppressing spurious alarms.
- A weighted composite risk index that fuses heterogeneous measurements into a graded alert, together with ventilation-based dilution and rock-stress relations used to set thresholds.
- A Monte-Carlo performance study comparing star, tree and mesh topologies and comparing the WSN with manual and wired monitoring.

II. LITERATURE SURVEY

2.1 Review of Existing Research and Methodologies

Akyildiz and Stuntebeck [3] identified the principal research challenges for wireless underground sensor networks: harsh channel conditions, energy constraints, topology design and the need for reliable multi-hop protocols. Yarkan et al. [8] surveyed underground-mine communication and grouped solutions into through-the-wire, through-the-air and through-the-earth approaches, while Forooshani et al. [9] reviewed measurement campaigns and propagation models for mine tunnels, showing that straight sections behave like lossy waveguides whereas bends and obstructions sharply increase attenuation.

Li and Liu [5] reported a structure-aware WSN for underground coal-mine monitoring that accounts for the long, narrow tunnel structure and the possibility of partial network failure after roof collapse. Moridi et al. [6] analysed the performance of star, tree and mesh ZigBee topologies for underground monitoring and communication, and later [7] integrated a ZigBee network with a geographic information system for mine monitoring. Bandyopadhyay et al. [12] described RFID- and ZigBee-based sensor networking for Indian underground mines, including personnel tracking.

For alternative physical layers, Sun and Akyildiz [10] examined magnetic-induction communication, which suffers little from soil and rock variability but offers limited range and bandwidth. Chehri et al. [11] investigated ultra-wideband (UWB) sensor networks for localisation in mining environments. Misra et al. [4] discussed safety-assurance and rescue-communication systems for high-stress environments and emphasised resilience and post-disaster operation. Surveys by Yick et al. [13] and

Gungor and Hancke [14] provide the general WSN and industrial-WSN design principles on which most of the above systems build.

2.2 Analysis of Existing Technologies and Comparison of Findings

Table 1: Comparison of representative previous studies

Study	Technology / focus	Key finding or contribution	Limitation relevant to this work
Li & Liu [5]	Structure-aware coal-mine WSN	Topology and protocol adapted to tunnel structure and failures	Focus on structure; limited multi-parameter risk fusion
Moridi et al. [6]	ZigBee star / tree / mesh comparison	Topology strongly affects performance in tunnels	Does not model alarm latency or energy jointly
Moridi et al. [7]	ZigBee + GIS	Integrated monitoring and communication with spatial display	Alarm logic mostly threshold-based
Sun & Akyildiz [10]	Magnetic induction	Channel stable in soil/rock	Short range, low data rate
Chehri et al. [11]	UWB localisation	Accurate positioning in mines	Not a complete safety-monitoring system
Forooshani et al. [9]	Propagation survey	Waveguide effect in straight tunnels; strong bend loss	Models need calibration per mine
Misra et al. [4]	Safety and rescue communication	Resilience and post-accident operation required	Conceptual; limited quantitative results

2.3 Research Gaps and Limitations

- Most studies address either communication performance or sensing, but few link network behaviour (loss, delay, energy) quantitatively to alarm performance.
- Alarm decisions are mostly single-parameter thresholds; multi-parameter fusion with false-alarm control is rarely quantified.
- Energy models seldom distinguish sensing energy of gas sensors, which dominates in methane nodes, from radio energy.
- Ventilation relations and rock-stress considerations are rarely used explicitly to derive alarm thresholds and sensor placement.

III. PROBLEM STATEMENT

The specific problem addressed is the design of an underground monitoring system that detects the onset of hazardous gas accumulation, oxygen depletion, abnormal heating and ground movement within seconds, delivers the information reliably over multi-kilometre roadways, survives partial damage, and operates for months on intrinsically safe batteries without generating a nuisance-alarm burden.

Table 2: Limitations of conventional monitoring and the need for an improved approach

Aspect	Conventional method (manual / cabled)	Required improvement
Sampling	Periodic rounds (e.g. every 30 min) or 30–120 s scan cycles	Continuous, event-adaptive sampling at seconds level

Aspect	Conventional method (manual / cabled)	Required improvement
Coverage	Sparse fixed points; faces and goafs poorly covered	Dense, quickly re-deployable nodes
Resilience	Single cable failure isolates sensors	Self-healing multi-hop mesh with alternate paths
Cost of change	Cable laying and relocation at each face advance	Battery nodes moved with the face
Alarm quality	Single threshold; false alarms from spikes	Filtering, confirmation and multi-parameter fusion
Data use	Mostly alarms; limited trend analysis	Time-series database, risk index and ventilation feedback

The technical challenges are (i) high and variable path loss in tunnels, (ii) energy-hungry gas sensors under intrinsic-safety limits, (iii) latency and reliability of multi-hop delivery along a linear topology, (iv) sensor drift, cross-sensitivity and noise, and (v) integration with ventilation and power-isolation practice. Operational challenges include rapid re-deployment, maintenance, calibration intervals and acceptance by the workforce and regulator.

IV. 4. OBJECTIVES OF THE STUDY

Primary objective: To design and evaluate a WSN-based system for real-time safety and environmental monitoring of underground mines.

Secondary objectives:

1. To identify the critical hazard parameters, sensing technologies and alarm thresholds for an underground mine.
2. To model radio propagation, multi-hop delivery and energy consumption in a tunnel environment.
3. To compare star, tree and mesh topologies on delivery ratio and transmission cost.
4. To quantify detection delay and false-alarm performance against manual and wired monitoring.
5. To develop a composite risk index and relate sensor thresholds to ventilation and rock-stress relations.

Expected technical improvements: detection delay reduced from minutes to seconds, extended coverage through self-healing mesh routing, lower false-alarm rate through confirmation logic, and battery life consistent with maintenance cycles. **Scope:** The study covers sensing, networking, alarm logic and analytical/simulation evaluation for a linear roadway of up to 2 km. Hardware field trials, through-the-earth links and full explosion-proof certification are outside the present scope.

V. PROPOSED METHODOLOGY

5.1 Description of the Proposed Approach

The proposed approach is a hierarchical WSN. Sensing nodes mounted on the roof or rib measure gases, microclimate and strata convergence and forward readings by IEEE 802.15.4 [15] to relay nodes that form a self-organising mesh toward an underground gateway. Routing follows an on-demand distance-vector principle [16] with link-quality metrics, so alternate relays are used when a link fails. The gateway connects to the surface by optical fibre or industrial Ethernet, where a server stores the data, evaluates alarm rules and the risk index, and drives dashboards, audible/visual alarms and ventilation or power-isolation interfaces. The methodology follows the workflow in Fig. 1.

5.2 Selection of Sensing Techniques and Components

Sensor selection is driven by the hazard, the required range and the permissible power. Methane is measured by non-dispersive infrared (NDIR) elements, which are stable and resistant to poisoning; CO, O_2 and H_2S are measured by electrochemical cells, which have very low power demand; temperature and relative humidity by digital sensors; and roof convergence by a wireless-enabled extensometer. Table 3 lists the monitored parameters and the illustrative alert levels adopted in this study. Statutory limits differ among countries and mines, so actual deployment must use the limits of the governing regulation.

Table 3: Monitored parameters, sensing technique and illustrative alert levels

Parameter	Sensing technique	Range	Safe level	Alarm level	Sampling (normal / alert)
Methane (CH_4)	NDIR	0–5 % v/v	≤ 0.5 %	1.0 % warning; 1.25 % evacuate	30 s / 5 s
Carbon monoxide (CO)	Electrochemical	0–500 ppm	≤ 5 ppm	50 ppm	30 s / 10 s
Oxygen (O_2)	Electrochemical	0–25 % v/v	20.9 %	≤ 19.5 %	60 s / 10 s
Carbon dioxide (CO_2)	NDIR	0–5 % v/v	≤ 0.1 %	0.5 %	60 s / 10 s
Air temperature	Digital sensor	0–60 °C	≤ 28 °C	37 °C	60 s / 20 s
Roof convergence rate	Extensometer	0–100 mm	≤ 0.1 mm/h	2 mm/h	300 s / 60 s

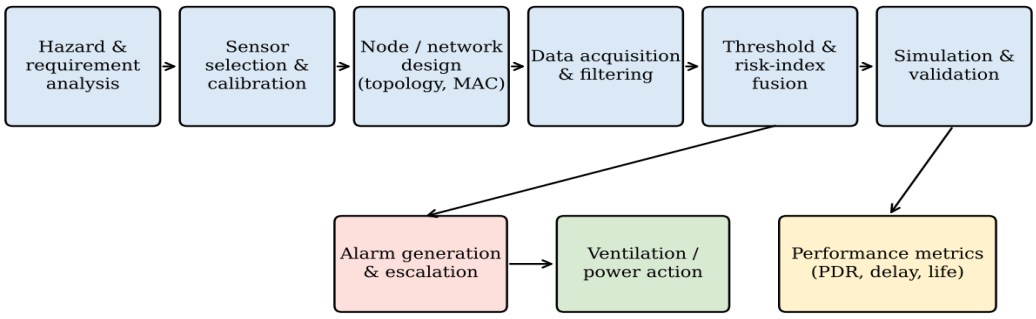


Fig. 1: Research methodology and workflow of the proposed monitoring system

5.3 Analytical and Simulation Procedure

The evaluation was carried out in four steps. (1) The tunnel link is characterised by a log-distance path-loss model with log-normal shadowing and converted to a per-attempt link-success probability. (2) A Monte-Carlo packet-level simulation of a linear roadway with a gateway at one end computes the delivery ratio and number of transmissions for star, tree and mesh forwarding. (3) A node-level energy model gives battery life for different node types and sampling intervals. (4) A time-domain methane-

release scenario is simulated 3,000 times with random sampling phase to compute detection delay, and a multi-hazard scenario is used to exercise the composite risk index.

5.4 Data Collection and Processing

Each node samples its sensors at the interval of Table 3, applies a first-order exponential filter and compares the filtered value with local thresholds. When a reading exceeds the advisory level the node switches to its faster alert sampling interval. Packets carry node identifier, timestamp, sensor values and battery state. At the server, data are time-stamped, validated against physical ranges, stored, and processed for trend, rate-of-change and the composite risk index.

5.5 Evaluation and Validation

Performance is judged by packet delivery ratio (PDR), transmissions per delivered packet, detection delay (mean and 95th percentile), false-alarm rate, estimated battery life and risk-index lead time. The simulation parameters are given in Table 4. Analytical results are cross-checked against closed-form expressions (Eqs. 3–5 and 10), and field validation with calibrated reference instruments is identified as future work.

Table 4: Simulation parameters

Parameter	Value
Carrier frequency / standard	2.4 GHz, IEEE 802.15.4
Transmit power / receiver sensitivity	0 dBm / −95 dBm (link budget 95 dB)
Reference loss PL(d_0), d_0 = 1 m	40.05 dB (free space)
Path-loss exponent n (obstructed tunnel)	3.0 (straight LOS: 1.9; heavy obstruction: 3.4)
Shadowing standard deviation σ	6 dB
Node spacing / roadway length	50 m / 2 km (40 nodes)
MAC retransmission attempts per hop	3
Supply / battery	3.3 V; 2 × 3 Ah lithium cells, 80 % usable, 2 %/yr self-discharge
Radio currents (Tx / Rx / sleep)	25 mA / 25 mA / 2 µA
NDIR methane sensing energy	132 mW for 1 s per sample
Methane scenario	0.30 % → 2.1 % ; τ = 420 s ; noise σ = 0.03 %
Monte-Carlo runs	3,000 (detection); 20,000 packets per point (PDR)

VI. SYSTEM ARCHITECTURE

Fig. 2 shows the overall architecture. The underground segment comprises sensing nodes, relay nodes forming a mesh backbone, wearable tags for personnel localisation, and the gateway. The surface segment comprises the control-room server, risk analytics, human–machine interface and the ventilation and power-control interface. The wired fibre/Ethernet link between gateway and surface carries aggregated data and avoids multi-kilometre radio hops to the surface.

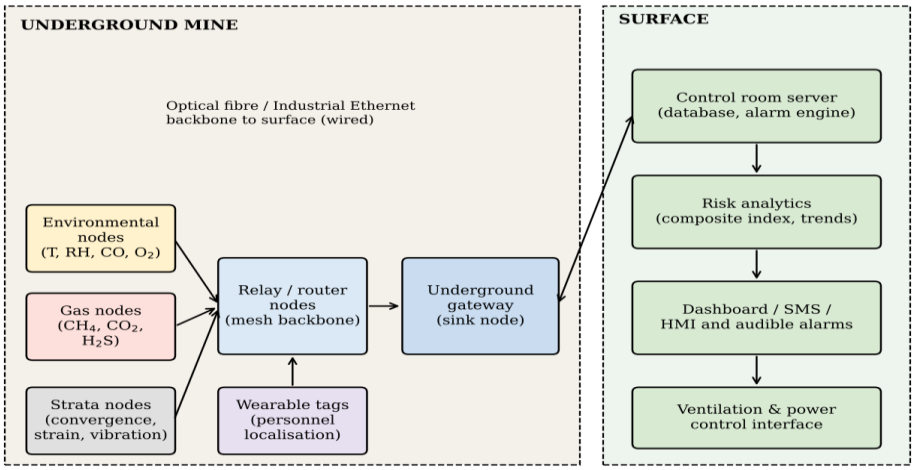


Fig. 2: Overall architecture of the WSN-based underground mine monitoring system

A sensing node (Fig. 3) integrates the sensors, signal conditioning and a 12-bit analogue-to-digital converter, a low-power microcontroller that performs filtering, local threshold comparison and adaptive sampling, an IEEE 802.15.4 transceiver, and an intrinsically safe battery pack. Relay nodes are placed at about 50 m spacing, staggered on alternate ribs where possible, so that each node has at least two forwarding candidates. Gas nodes are installed near the roof where methane accumulates, CO and temperature nodes in return airways and near conveyors and goaf edges, and strata nodes in the junctions and the face-end roadway.

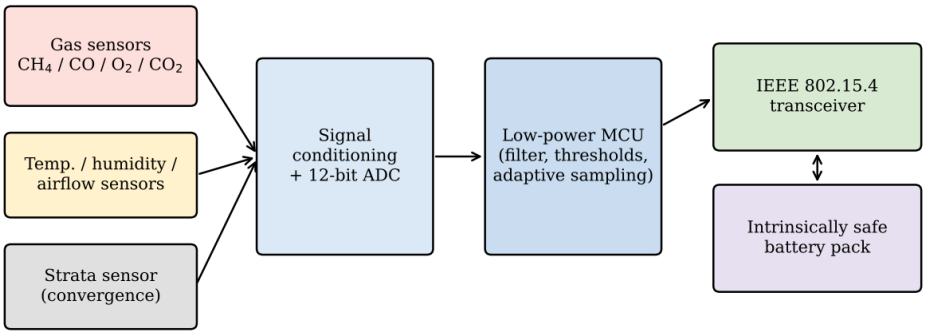


Fig. 3: Block diagram of a sensing node

VII. MATHEMATICAL MODELLING AND TECHNICAL ANALYSIS

7.1 Radio Propagation in the Tunnel

The mean path loss at distance d is described by the log-distance model with log-normal shadowing [17]:

$$PL(d) = PL(d_0) + 10\,n \log_{10}\left(\frac{d}{d_0}\right) + X_\sigma \quad (1)$$

where n is the path-loss exponent and X_σ is a zero-mean Gaussian variable with standard deviation σ (dB). The reference loss at d_0 = 1 m is the free-space value

$$PL(d_0) = 20 \log_{10}\left(\frac{4\pi d_0}{\lambda}\right) \quad (2)$$

With a 95 dB link budget, the mean range is d = 10^((95 − 40.05)/(10n)), giving about 780 m for a straight line-of-sight tunnel (n = 1.9), 68 m for an obstructed tunnel (n = 3.0) and 41 m for heavy obstruction (n = 3.4) (Fig. 4). The probability that a single transmission succeeds at distance d is

$$p(d) = \Phi\left(\frac{PL_{\max} - PL_{\mathrm{m}}(d)}{\sigma}\right) \quad (3)$$

where Φ is the standard normal distribution function, PL_{max} is the link budget and PL_m the mean loss of Eq. (1). For the parameters of Table 4, p(50 m) = 0.746, p(100 m) = 0.200 and p(150 m) = 0.043.

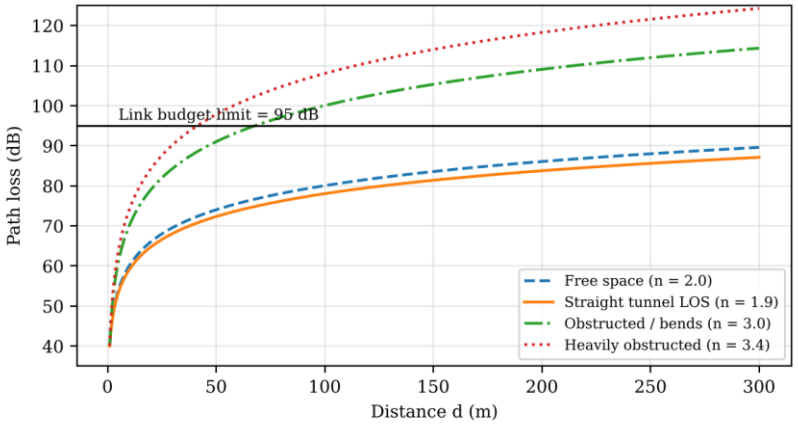


Fig. 4: Path loss versus distance for different tunnel conditions and the 95 dB link-budget limit

7.2 Multi-Hop Delivery

With R MAC attempts per hop, the probability that a hop succeeds is

$$P_{\text{hop}} = 1 - (1 - p)^R \tag{4}$$

and the end-to-end packet delivery ratio over h hops is the product of the hop probabilities:

$$\text{PDR} = \prod_{i=1}^{h} P_{\text{hop},\, i} \tag{5}$$

For mesh forwarding, a failed attempt to the next node is followed by an attempt to the node two positions ahead, which raises P_{hop} at the cost of extra transmissions.

7.3 Energy Consumption and Lifetime

The average power drawn by a node with sampling interval T_s is

$$P_{\text{avg}} = \frac{E_s + E_{\text{tx}} + E_{\text{rx}}}{T_s} + P_{\text{sleep}} + D_L\, P_{\text{rx}} \tag{6}$$

where E_s is the sensing energy per sample, E_{tx} and E_{rx} are the radio energies for sending a packet and receiving its acknowledgement, P_{sleep} includes sleep and self-discharge power, and $D_L\, P_{\text{rx}}$ is the idle-listening cost of a relay with listening duty cycle D_L [18]. The battery lifetime follows from

$$L = \frac{\eta\, E_{\text{bat}}}{P_{\text{avg}}} \tag{7}$$

with η the usable fraction of the battery energy. Because an NDIR methane element draws about 132 mW during its warm-up, E_s dominates for methane nodes, whereas radio energy dominates for relays.

7.4 Detection Delay and False-Alarm Control

The delay between the true crossing of a threshold and the alarm at the control room is

$$T_{\text{det}} = T_{\text{wait}} + T_{\text{conf}} + T_{\text{net}} + T_{\text{proc}} \tag{8}$$

where T_{wait} is the time to the next sample (mean $T_s/2$ for random phase), T_{conf} is the time for confirmation samples, T_{net} the network latency and T_{proc} the processing time. Each node smooths readings with a first-order filter

$$\hat{x}_k = \alpha\, x_k + (1 - \alpha)\, \hat{x}_{k-1} \tag{9}$$

with $0 < \alpha \leq 1$. If an isolated spurious reading exceeds the threshold with probability p per sample, a two-out-of-three confirmation rule produces a false alarm with probability

$$P_{\text{FA}} = 3p^2 - 2p^3 \tag{10}$$

For p = 10^{-3} and 30 s sampling (2,880 samples per day), single-sample triggering gives 2.88 false alarms per node per day, while Eq. (10) gives 0.0086 per node per day.

7.5 Mine Ventilation Calculations

The airflow needed to dilute a methane emission of q (m³/s) to a permitted concentration C_p (as a fraction) in the return air is [1]

$$Q = \frac{q}{C_p} \tag{11}$$

The frictional pressure drop in a roadway of perimeter P, length L and cross-sectional area A carrying airflow Q follows Atkinson's law:

$$\Delta p = \frac{k P L Q^2}{A^3} \tag{12}$$

Worked example. For a methane emission of q = 3 m³/min (0.05 m³/s) and C_p = 0.75 % (0.0075), Eq. (11) gives Q = 6.67 m³/s. For an arched roadway with A = 12 m², P = 14 m, L = 1,500 m, k = 0.012 N·s²/m⁴ and Q = 10 m³/s, Eq. (12) gives Δp = 0.012 × 14 × 1500 × 10² / 12³ = 14.6 Pa. Fig. 5 shows the dilution relationship; a sudden rise of return-air CH_4 detected by the WSN indicates either increased emission or reduced airflow, and the ventilation controller can distinguish the two using airflow nodes.

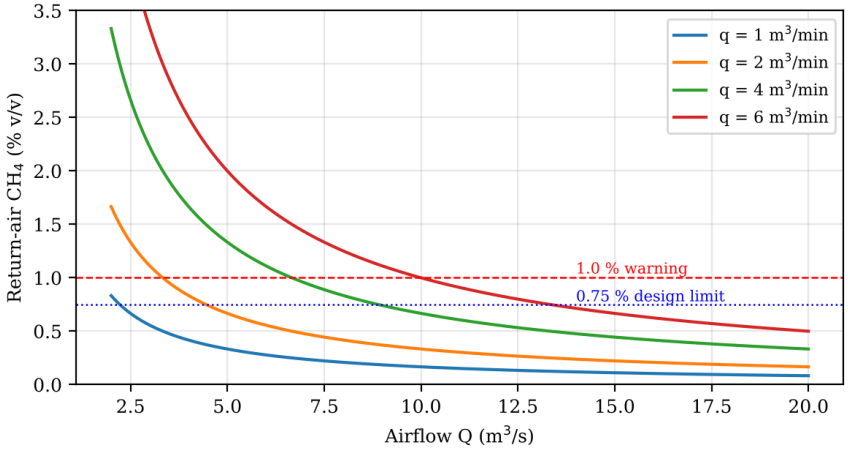


Fig. 5: Return-air methane concentration versus airflow for different gas emission rates

7.6 Rock Stress and Strata Monitoring

The vertical in-situ stress at depth H in rock of unit weight γ is $\sigma_v = \gamma H$; for γ = 25 kN/m³ and H = 400 m, σ_v = 10 MPa. Roof and rib deformation is monitored through strain and convergence rate:

$$\varepsilon = \frac{\Delta L}{L_0}, \qquad v_c = \frac{\Delta \delta}{\Delta t} \tag{13}$$

where ΔL is the change of the gauge length L_0, Δδ is the change of roof-to-floor convergence over time Δt, and v_c is the convergence rate. An accelerating v_c, rather than the absolute displacement alone, is the more reliable precursor of instability, and the alert level of 2 mm/h in Table 3 is therefore expressed as a rate.

7.7 Composite Risk Index

Each parameter i is normalised between its safe value x_{safe} and alarm value x_{alarm}:

$$s_i = \min\left\{1,\ \max\left\{0,\ \frac{x_i - x_{\text{safe},i}}{x_{\text{alarm},i} - x_{\text{safe},i}}\right\}\right\} \tag{14}$$

and the composite index is the weighted sum

$$R = \sum_i w_i s_i, \qquad \sum_i w_i = 1 \tag{15}$$

with weights 0.30 (CH_4), 0.25 (CO), 0.15 (O_2), 0.10 (temperature) and 0.20 (roof convergence rate). The levels adopted are Normal ($R < 0.3$), Caution ($0.3 \leq R < 0.6$), Warning ($0.6 \leq R < 0.8$) and Danger ($R \geq 0.8$). The weights are engineering judgements for this study and should be tuned for each mine from its hazard assessment.

VIII. RESULTS AND DISCUSSION

Note on results. The results in this section were obtained from the analytical models and Monte-Carlo simulation described above, using the assumed parameters of Table 4. They characterise design trade-offs and are not field measurements.

8.1 Network Performance by Topology

Table 5: Packet delivery ratio and transmissions per delivered packet versus distance from the gateway

Distance (m)	Hops	PDR star (%)	PDR tree (%)	PDR mesh (%)	Tx / packet tree	Tx / packet mesh
50	1	74.6	98.2	98.5	1.3	1.6
100	2	20.0	96.8	97.6	2.6	3.1
200	4	0.9	93.7	96.0	5.2	6.0
400	8	< 0.1	87.9	93.1	10.0	11.6
600	12	< 0.1	82.2	90.1	14.4	17.0
800	16	< 0.1	77.1	87.3	18.7	22.3
1000	20	< 0.1	71.7	84.7	22.6	27.4
1500	30	< 0.1	61.7	78.3	31.6	39.5
2000	40	< 0.1	51.5	72.9	38.8	50.8

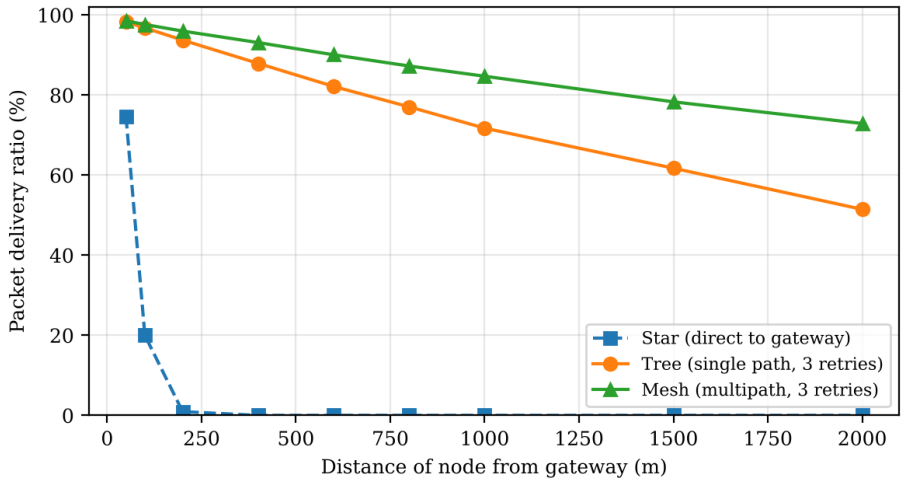


Fig. 6: Packet delivery ratio versus distance from the gateway for star, tree and mesh forwarding

Star topology (direct transmission) is not viable: even at 100 m the delivery ratio is 20.0% and beyond about 200 m it is negligible. Multi-hop forwarding is essential in obstructed tunnels. The single-path tree degrades with the number of hops, reaching 51.5% at 2 km, because every hop is a point of loss. Mesh forwarding with a two-node-ahead alternate keeps 72.9% at 2 km, an improvement of 21.4 percentage points, at the cost of about 31% more transmissions per delivered packet. This agrees qualitatively with the topology comparisons reported for ZigBee networks in tunnels [6]. For safety-

critical alarm packets this reliability gain justifies the additional energy, and application-layer acknowledgement or redundant gateway paths can be used to approach 100%.

8.2 Energy and Node Lifetime

Table 6: Estimated battery life (days) versus sampling interval

Node type	10 s	30 s	60 s	120 s	300 s	600 s
Environmental (T, RH, CO, O_2)	2427	> 3650	> 3650	> 3650	> 3650	> 3650
Methane NDIR, leaf node	45	135	267	524	1246	2304
Methane NDIR + relay (2 % listening)	39	96	152	213	280	313

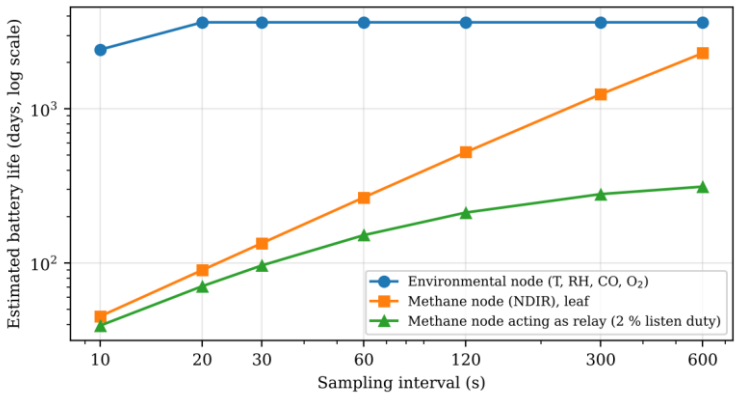


Fig. 7: Estimated battery life versus sampling interval for different node types

Environmental nodes using electrochemical sensors reach the cell shelf life at intervals of 20 s or longer. NDIR methane nodes are limited by sensing energy: at a 30 s interval a leaf node lasts about 135 days and a relay-capable methane node about 96 days on the assumed battery. This indicates that critical methane nodes should either use a larger intrinsically safe battery pack, a lower-power sensing element, or a wired power backbone, while relay duty should be given to environmental nodes, which have a large energy margin. Adaptive sampling (30 s normally, 5 s only during an alert) preserves lifetime because alert intervals are rare.

8.3 Methane Detection Performance

Fig. 8 shows a simulated methane build-up from 0.30 % to 2.1 %, crossing the 1.0 % warning level at 23.4 min. Because the node switches to 5 s sampling once the reading exceeds 0.5 %, the 1.0 % level is confirmed quickly even in the presence of sensor noise.

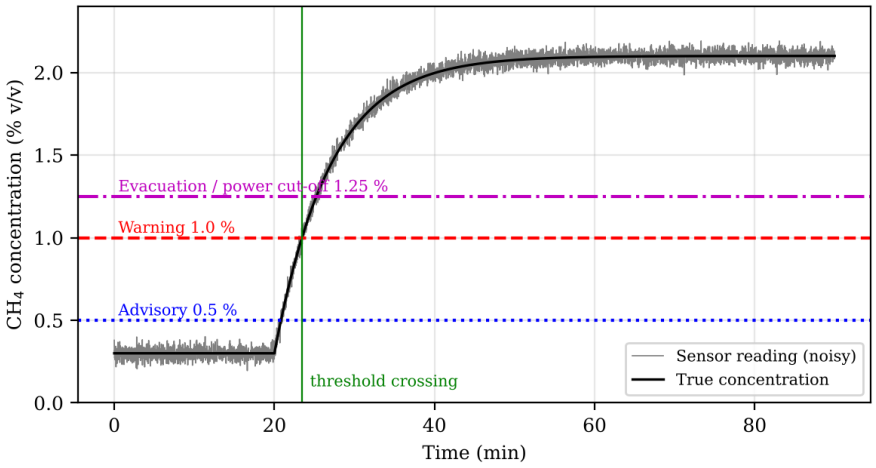


Fig. 8: Simulated methane build-up, sensor readings and alert thresholds

Table 7: Detection delay for the 1.0 % methane warning level (3,000 runs)

Monitoring method	Mean delay (s)	95th percentile (s)	Maximum (s)
Manual rounds every 30 min	952	1764	1873
Wired telemetry, 60 s poll, 2 consecutive readings	92.0	126.0	152.0
Proposed WSN, adaptive 5–30 s, 2-of-3 confirmation	7.4	19.4	31.3

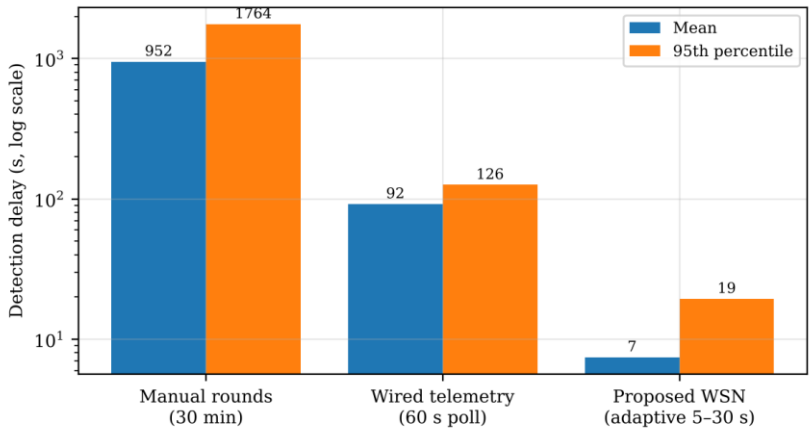


Fig. 9: Comparison of detection delay for manual, wired and WSN-based monitoring

The proposed WSN detects the warning level with a mean delay of 7.4 s (95th percentile 19.4 s), a reduction of 92% relative to wired polling and 99.2% relative to manual rounds. Manual rounds, with a mean delay of 15.9 min and a worst case near 31 min, would leave a methane build-up undetected for most of its rise. The two-out-of-three confirmation reduces the expected false alarms from 2.88 to 0.009 per node per day for a spurious-reading probability of 10^{-3} (Eq. 10), while adding only two short alert-mode samples to the delay.

8.4 Composite Risk Index

A one-hour multi-hazard scenario was simulated in which CO and temperature begin to rise at 22 min (heating), methane begins to accumulate at 25 min, oxygen declines slowly and roof convergence accelerates from 35 min. Fig. 10 shows the individual scores and the composite index. The index crosses the Caution level at 29.3 min, the Warning level at 36.3 min and the Danger level at 46.3 min. No single parameter reached its own alarm level until later in the sequence, so the fused index gave an earlier, graded and more interpretable alert than independent single-parameter thresholds, and CO and temperature rise supplied the earliest evidence of heating.

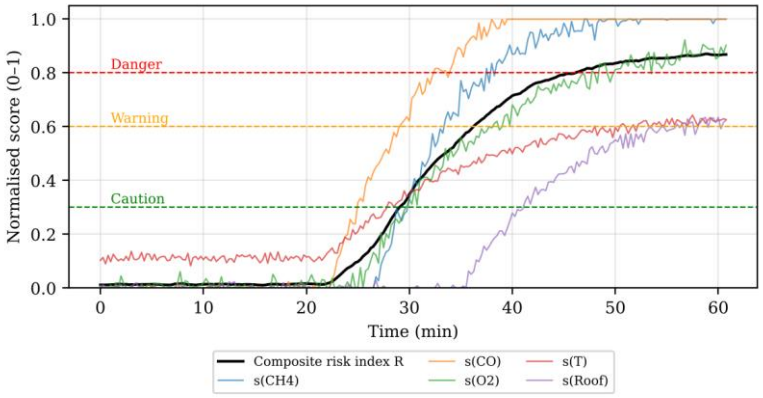


Fig. 10: Individual parameter scores and composite risk index for a simulated multi-hazard scenario

8.5 Comparison with Existing Methods

Table 8: Summary comparison of monitoring approaches

Feature	Manual rounds	Wired telemetry	Proposed WSN
Mean detection delay (methane)	15.9 min	92 s	7.4 s
Spatial density	Low	Medium	High
Re-deployment at face advance	Not applicable	Slow, costly	Fast, low cost
Failure tolerance	Human dependent	Cable cut isolates nodes	Mesh re-routing
Alarm logic	Reading by person	Single threshold	Filter + confirmation + risk index
Main limitation	Intermittent	Fixed infrastructure	Battery and channel limits

The results show that the WSN's principal advantages are speed, density and resilience, whereas its principal limitations are battery life of gas nodes and the channel variability of the tunnel. Consistent with the literature [9], [10], the design therefore treats link margin and relay placement as primary design variables and relies on a wired backbone from gateway to surface. These conclusions rest on a simulated channel; the path-loss exponent and shadowing must be calibrated with measurements from the target mine before deployment.

IX. CONCLUSION

This paper described the architecture, analytical models, and simulation-based assessment of a wireless sensor network for underground mine safety and environmental monitoring. Its key findings are as follows.

• Direct (star) communication is impractical in obstructed tunnels beyond roughly 100 m. Over a 2 km distance, a mesh network with alternate forwarding delivered 72.9% of packets, compared with 51.5% for a single-path tree.

• Adaptive sampling with confirmation logic detected methane warnings in an average of 7.4 s, compared with 92 s for wired polling and 15.9 min for manual rounds. Its false-alarm rate was more than two orders of magnitude lower.

• Gas-sensing energy use is the primary constraint on methane-node lifetime. These nodes should therefore use larger intrinsically safe battery packs or a wired backbone, whereas environmental nodes can operate for years.

• A composite risk index combined CO, temperature, CH_4, O_2, and convergence data into a graded alert that increased before any individual alarm threshold was reached.

The research objectives set out in Section 4 were thus achieved at the analytical and simulation levels. The principal technical contributions are an integrated network–sensing–alarm model, an adaptive alarm scheme with confirmation, and a risk-index framework linked to ventilation and rock-stress relationships. In practice, this approach can support faster withdrawal decisions, more targeted ventilation control, lower cabling costs at advancing faces, and a data record for post-incident analysis.

Future Scope

- Field trials in an operating mine with calibrated reference instruments to validate path-loss parameters, delay and false-alarm results.
- Explosion-proof and intrinsic-safety certification of node hardware and battery packs.
- Hybrid links combining 2.4 GHz mesh with sub-GHz, magnetic-induction or leaky-feeder links for through-bend and post-disaster survivability.
- Machine-learning-based anomaly detection and learned weights for the risk index using historical mine data.
- Integration with automatic ventilation control, personnel and vehicle tracking, and digital-twin visualisation.

REFERENCES

[1] M. J. McPherson, *Subsurface Ventilation and Environmental Engineering*. London, U.K.: Chapman & Hall, 1993.

[2] I. F. Akyildiz, W. Su, Y. Sankarasubramaniam, and E. Cayirci, “A survey on sensor networks,” *IEEE Commun. Mag.*, vol. 40, no. 8, pp. 102–114, Aug. 2002.

[3] I. F. Akyildiz and E. P. Stuntebeck, “Wireless underground sensor networks: Research challenges,” *Ad Hoc Netw.*, vol. 4, no. 6, pp. 669–686, Nov. 2006.

[4] P. Misra, S. Kanhere, D. Ostry, and S. Jha, “Safety assurance and rescue communication systems in high-stress environments: A mining context,” *IEEE Commun. Mag.*, vol. 48, no. 4, pp. 66–73, Apr. 2010.

[5] M. Li and Y. Liu, “Underground coal mine monitoring with wireless sensor networks,” *ACM Trans. Sens. Netw.*, vol. 5, no. 2, Art. 10, Mar. 2009.

[6] M. A. Moridi *et al.*, “Performance analysis of ZigBee network topologies for underground space monitoring and communication systems,” *Tunn. Undergr. Space Technol.*, vol. 27, no. 1, pp. 69–75, 2012.

[7] M. A. Moridi *et al.*, "Development of underground mine monitoring and communication system integrated ZigBee and GIS," *Int. J. Min. Sci. Technol.*, vol. 25, no. 5, pp. 811–818, 2015.

[8] S. Yarkan, S. Güzelgöz, H. Arslan, and R. R. Murphy, "Underground mine communications: A survey," *IEEE Commun. Surveys Tuts.*, vol. 11, no. 3, pp. 125–142, 3rd Quart. 2009.

[9] A. Forooshani, S. Bashir, D. G. Michelson, and S. Noghanian, "A survey of wireless communications and propagation modeling in underground mines," *IEEE Commun. Surveys Tuts.*, vol. 15, no. 4, pp. 1524–1545, 4th Quart. 2013.

[10] Z. Sun and I. F. Akyildiz, "Magnetic induction communications for wireless underground sensor networks," *IEEE Trans. Antennas Propag.*, vol. 58, no. 7, pp. 2426–2435, Jul. 2010.

[11] A. Chehri, P. Fortier, and P.-M. Tardif, "UWB-based sensor networks for localization in mining environments," *Ad Hoc Netw.*, vol. 7, no. 5, pp. 987–1000, Jul. 2009.

[12] L. K. Bandyopadhyay, S. K. Chaulya, and P. K. Mishra, *Wireless Communication in Underground Mines: RFID-Based Sensor Networking*. New York, NY, USA: Springer, 2010.

[13] J. Yick, B. Mukherjee, and D. Ghosal, "Wireless sensor network survey," *Comput. Netw.*, vol. 52, no. 12, pp. 2292–2330, Aug. 2008.

[14] V. C. Gungor and G. P. Hancke, "Industrial wireless sensor networks: Challenges, design principles, and technical approaches," *IEEE Trans. Ind. Electron.*, vol. 56, no. 10, pp. 4258–4265, Oct. 2009.

[15] *IEEE Standard for Local and Metropolitan Area Networks—Part 15.4: Low-Rate Wireless Personal Area Networks (LR-WPANs)*, IEEE Std 802.15.4-2011, Sep. 2011.

[16] C. Perkins, E. Belding-Royer, and S. Das, "Ad hoc on-demand distance vector (AODV) routing," IETF, RFC 3561, Jul. 2003.

[17] T. S. Rappaport, *Wireless Communications: Principles and Practice*, 2nd ed. Upper Saddle River, NJ, USA: Prentice Hall, 2002.

[18] W. R. Heinzelman, A. Chandrakasan, and H. Balakrishnan, "Energy-efficient communication protocol for wireless microsensor networks," in *Proc. 33rd Hawaii Int. Conf. Syst. Sci. (HICSS)*, Maui, HI, USA, Jan. 2000, pp. 1–10.

[19] W. B. Heinzelman, A. P. Chandrakasan, and H. Balakrishnan, "An application-specific protocol architecture for wireless microsensor networks," *IEEE Trans. Wireless Commun.*, vol. 1, no. 4, pp. 660–670, Oct. 2002.